Snow gliding and loading under two different forest stands: a case study in the north-western Italian Alps

TITLE: Snow gliding and loading under two different forest stands: a case study in the north-western Italian Alps.

AUTHORS: Davide Viglietti*, Margherita Maggioni, Enrico Bruno, Ermanno Zanini, Michele Freppaz

AFFILIATION: University of Torino - Dipartimento di Scienze Agrarie Forestali e Alimentari and NatRisk-LNSA
Via L. Da Vinci 44, 10095 Grugliasco (TO), Italy

CORRESPONDING AUTHOR: Davide Viglietti, e-mail: davide.viglietti@unito.it, Tel: +39 011 6708522, Fax: +39 011 6708692

Davide Viglietti, male, was born in Cuneo on 7th of June 1980. He is PhD graduated in Forestry and Environmental Sciences at University of Turin, Faculty of Agriculture.

ABSTRACT:

The presence of a thick snowpack could interfere with forest stability, especially on steep slopes with potential damages for young and old stands. The study of snow gliding in forests is rather complex because this phenomenon could be influenced not only by forest features, but also by snow/soil interface characteristics, site morphology, meteorological conditions and snow physical properties. Our starting hypothesis is that different forest stands have an influence on the snowpack evolution and on the temperature and moisture at the snow/soil interface, which, subsequently, could affect snow gliding processes and snow forces.

The study site is located in a subalpine forest in Aosta Valley (NW-Italy) and includes two plots at the same altitude, inclination and aspect but with different tree composition: Larch (*Larix decidua*) and Spruce (*Picea abies*). The plots were equipped with moisture and temperature sensors placed at the snow/soil interface (O horizon) and glide shoes for continuous monitoring of snow gliding. The recorded data were related to periodically monitored snowpack and snow/soil interface properties. Data were collected during two winter seasons (2009-10 and 2010-11). The snow forces on trees were analytically calculated either from snowpack data and site morphology or also from measured snow gliding rates.

Different snow accumulation were observed under the two different forest stands, with a significant effect on temperature and moisture at the snow/soil interface. The highest snow gliding rates were observed under Larch and were related to rapid increases of moisture at the snow/soil interface. The calculated snow forces were generally lower than the threshold values reported for tree uprooting due to snow gliding, as confirmed by the absence of tree damages in the study areas.

KEY WORDS: snow/soil interface; temperature; water content; snow forces; trees

1. Introduction

Snow forces are a result of glide and creep processes of the snowpack: a) snow gliding is the slow downhill motion of the snow on the ground mainly influenced by the roughness of the ground surface and the wetness of the lowermost boundary layer of the snow cover; b) snow creep is the result of settlement and internal shear deformation parallel to the slope (In der Gand and Zupancic 1966).

The snow gliding is strictly dependent on physical snow characteristics, overall depth, density and moisture, and on morphological features, overall slope angle and surface roughness (McClung and Larsen 1989; Jones, 2004; Margreth 2007; Höller et al. 2009). In the first period of extensive research of glide processes and glide avalanches, Bader at al. (1939) found that the most important factors that have an effect on glide are slope exposure, degree of surface roughness, temperature at the ground surface and the thickness and properties of the snow cover. They proposed that the primary action of these factors is their effect on the frictional conditions of the slide surface. Basal friction is obviously reduced by the presence of liquid water at the snow/soil interface (McClung and Clarke, 1987). Also Clarke and McClung (1999) stated that gliding can occur if 1) the interface is smooth (e.g. bare rock or grassy vegetation), 2) the temperature at the snow/ground interface is at 0º C, guaranteeing the presence of free water at the interface, and 3) the slope angle is at least 15º for roughness typical of alpine ground cover. Moreover, the intensity of gliding rates is strictly related to increases in snow/soil interface temperature and moisture (Lackinger 1987; McClung and Larsen 1989; Clarke and McClung 1999; Newesely et al. 2000).

The wide-scale analysis of snow gliding intensity in alpine and subalpine areas has to take into account the land-use changing: the abandonment of pastures and the natural afforestation could cause a significant change on the ground roughness. In particular, Newesely et al. (2000) found that the abandonment of agriculture land may foster an increase of snow gliding rates due to the reduction of basal frictions.

Although forests can reduce the snow gliding intensity (Leitinger et al. 2008) by preventing snow accumulation and homogeneous snow distribution due to interception and falling of snow from the crowns (Höller 1995, 2001), it is not possible to totally exclude snow gliding in forest. Snow gliding might have significant effects on forest plants; in particular, juvenescent trees might be uprooted from the ground or the growth of young plants might be strongly affected by the snow forces (In der Gand 1978). According to these evidences, Höller et al. (2009) evaluated, with different approaches, the snow gliding rates in an Austrian subalpine stand of small trees (*Pinus cembra*, *Larix decidua* and *Picea abies*). In the same work, snow forces measured in field, and back-calculated with different equations, were compared to the forces necessary to uproot the young trees: the authors measured that forces equal to 950 N and 3500 N can uproot juvenescent trees with a diameter of 0.02 m and 0.045 m, respectively.

The study of the snow gliding phenomenon in forests is rather complex because it is influenced not only by forest features (species, crown, diameter and density), but also by site (slope angle, morphology, aspect), meteorological (air temperature, rain on snow events) characteristics and snowpack structure. Moreover, the impact of snow forces on trees depends on the forest characteristics itself, and it could lead to different consequences in term of tree stability.

The aim of this work is to analyse the snowpack evolution and snow gliding movements under different forest covers Larch (*Larix decidua*) and Spruce (*Picea abies*) stands, in order to determine the snow forces acting on trees of different species and diameters. In particular, we aim at evaluating the influence of physical properties as temperature and moisture at the snow/soil interface on snow gliding processes, and consequently on snow forces.

2. Methodology

2.1. The study site

As this research was developed within the project “Forêts de protection: techniques de gestion et innovation dans les Alpes occidentals” in the frame of the Operational Program ALCOTRA Italy-France (2009-2012), the study site was chosen within a snow avalanche protection forest. It is located in the Municipality of Brusson, in the Aosta Valley Region (North Western Italian Alps), at an elevation of 1950 m a.s.l. It is characterized by a south aspect and a mean slope angle of about 40°. The coniferous mixed forest of the study site is mainly composed of larch (*Larix decidua*), spruce (*Picea abies*) with a lower presence of pinus (*Pinus uncinata*). The lower part of the forest was reforested in 1940, in order to protect the village beneath, and it was pastured.

The climate of the area is continental humid subarctic, with a mean annual air temperature equal to + 4 °C and a mean annual precipitation equal to 718 mm. The mean annual snow depth is 175 cm (Mercalli et al. 2003).

Two adjacent plots (40x40 m), located at the same elevation and aspect, were chosen (Fig. 1): a) one within a larch stand (Larch plot) and b) another one within a spruce stand (Spruce plot). By counting all trees in each plot (with stem diameter > 5 cm) the average stem density was determined equal to 300 stems/ha for both plots. The crown canopy, measured as crown projection, amounted to 60% for the Larch plot and 65% for the Spruce plot. The average stem diameter was 40 cm and the most of the trees were included in the range 30 - 40 cm (10 cm interval). The natural regeneration was generally scarce.

2.2 Data collection

At the snow/soil interface (O horizon) each plot was equipped with thermistor probes, with accuracy of ±0.1 ºC, (MadgeTech®) and volumetric moisture probes, which measure the dielectric constant of the media through the utilization of capacitance/frequency domain technology, with

accuracy of ±3 % VWC, (EC-5MadgeTech). Temperature and moisture measured at snow/soil interface were named respectively as Ti and Mi.

Moreover, two glide shoes connected to potentiometers (Sommer®) (Fig. 2) as developed by in In der Gand (1954) and successively applied by other scientists (e.g. Leitinger et al. 2008; Höller et al. 2009), were placed in each plot at a minimum distance of 5 m below the first upwards tree. The potentiometers were calibrated in order to convert the electric signal registered by the snow shoes into downward movement (mmd^{-1}), caused by snow gliding. All sensors were connected with a central data logger (Datataker® DT-80) supplied by a long duration battery and set to record the different parameters every 15 minutes. The electric wires were cabled underground in order to minimize their effect on the surface roughness.

The meteorological data were acquired by an automatic snow and weather station closed to the site (Gressoney-Weissmetten 2038 m a.s.l.) belonging to the Ufficio Centro Funzionale of the Aosta Valley Region.

The snowpack physical characteristics (snow depth -H_S-, snow density -ρ-, grain types and size, snow temperatures, hand hardness index) were measured monthly, following standard international methods (Fierz et al., 2009): 8 snow profiles in winter 2009-10 and 3 snow profiles in winter 2010-11 were done in both plots. The damages to the trees were evaluated in the field by observations of eventual uprooted trees and broken branches at the end of winters.

Data collection was done from the middle of November 2009 until the end of April 2010 (called winter 2009-10) and from the middle of November 2010 until the end of April 2011 (called winter 2010-11). The seasons were identified according to meteorological quarterly subdivision: fall included September, October, November; winter included December, January and February; spring included March, April and May.

2.3 Calculation of snow forces

The calculation of snow forces on stems was done following the approach used by Höller et al. (2009). In particular, two different methods were applied by using a) empirical equations (Margreth et al., 2007) - see section 2.3.1 - and b) snow gliding data recorded with glide shoes (Mc Clung and Larsen, 1989) - see section 2.3.2. We calculated snow forces for different stem diameters (0.02, 0.05, 0.1, 0.2, 0.3, 0.4, 0.5 m) in order to consider the real diameter distribution observed in the field and to compare our results with the available literature.

2.3.1 Snow pressure according to the Swiss guidelines

Margreth et al. (2007) applied the Swiss Guidelines with some improvements in order to calculate snow pressure on cableway masts. The snow pressure was calculated with the following equation (Eq.1):

Eq.1 $$S'_N = \rho g(H_S^2/2)KN$$

where:

S'_N is the snow pressure component in the line of slope per meter run of the supporting surface along the contour line [kNm^{-1}];

ρ is the density of the snow cover [tm^{-3}];

g is the gravitational acceleration [ms^{-2}];

H_S is the vertical snow depth [m];

K is the creep factor dependent on the slope inclination ψ and the density ρ;

N is the glide factor.

164 In Margreth et al. (2007) the *K* factor was associated to fixed snow density values. We interpolated
165 those values in order to calculate the exact *K* factor from the snow density that we measured in the
166 field ($y = 0.73\ x + 0.547$, $r^2 = 0.991$, where y corresponds to $K/\sin 2\psi$ and x to ρ). After that, $K/\sin 2\psi$
167 was multiplied by $\sin 2\psi$ (where ψ corresponds to the inclination of the study site).
168 In Margreth et al. (2007), the *N* factor depends on the ground roughness and aspect: it increases
169 from WNW-N-ENE to ENE-S-WNW and it is inversely related to the ground roughness. Forest is
170 not a determining parameters in the choice of *N*. Therefore, in our forested plots, we used the
171 ground class 1, assuming that stems determined a high surface roughness (more than boulders). The
172 study site was included in the ENE-S-WNW aspect class, because it is located on a South slope.
173 Finally, we chose a glide factor *N* equal to 1.3.
174 Equation 1, which is valid only for infinitely long planes, was integrated, as suggested by Margreth
175 et al. (2007), with a coefficient (η_F), in order to consider the end-effect forces on narrow obstacles.
176 η_F was calculated with the following equation (Eq. 2):
177
178 **Eq.2** $\eta F = 1+c(D/W)$

179 where:
180 *D* is the snow thickness (calculated as $H_S * \cos\psi$, where H_S is the vertical snow depth measured in the
181 field and ψ is the slope angle);
182 *W* is the width of the structure (that corresponded to the stem diameter);
183 *c* is a non-dimensional coefficient and depends on the snow gliding intensity. It is usually deduced
184 from the Swiss Guidelines. We used the smallest coefficient (c = 0.6) because the snow gliding is
185 typically low in dense forest areas (Höller 2001).
186 Subsequently, equations1 and 2 were joined in equation 3:
187

188 **Eq.3** $S'_{N,M} = \rho g(H_S^2/2)KN\eta_F(W/D)$

189

190 Finally, the snow pressure $S'_{N,M}$ was multiplied by the different stem diameter classes in order to
191 compare our results, in term of forces, with those presented by Höller et al. (2009).

192

193 2.3.2 Snow pressure according to Mc Clung and Larsen (1989)

194 This method considered the snow gliding rates directly measured in the field to determine principal
195 stress on structures in dependence of the stagnation depth:

196

197 **Eq.4** $\sigma = \{[2/(1-\upsilon)]\ [(d'/D)+(L/HS)]\ \}0.5\ \rho gDsin\psi+0.5[\upsilon/(1-\upsilon)]\ \rho gDcos\psi$

198

199 where:

200 σ is the maximal principal stress of the snow on a structure [Nm^{-2}];

201 υ is the Poisson coefficient deduced from Salm et al.(1971). We used υ = 0.1 that corresponds to a
202 mean snow density of 250 kgm^{-3}, equal to the density we measured in our plots;

203 L/H_S is a dimensionless creep parameter calculated by McClung and Larsen (1989) equal to 0.27 +
204 (υ/12);

205 D is the snow thickness;

206 ρ is the snow density measured in the field [kgm^{-3}];

207 g is the gravitational acceleration [ms^{-2}];

208 ψ is the slope angle;

209 d' is the stagnation depth.

The stagnation depth is a fundamental parameter to formulate the boundary condition at the snow/soil interface. We calculated the stagnation depth *d'* from the measured snow gliding rates using Equation 5 (McClung, 1974):

$$\textbf{Eq.5} \quad d' = [\mu V_g]/[2(1-\upsilon)\rho g D \sin\psi] \tag{5}$$

where:

μ is the viscosity, equal to 10^{11} Pa for snow;

V_g is the snow gliding velocity [mmd^{-1}]. According to Hoeller (2009) we used the maximum daily snow gliding rate recorded during winters 2009-10 and 2010-11;

υ is the Poisson coefficient.

2.4 Statistical analysis

Descriptive statistics were used to analyzed meteorological pattern, snow physical characteristics, and snow gliding data. Correlation analysis between temperature and moisture at snow/soil interface and between air temperature and temperature and moisture at snow/soil interface were carried out using the SPSS 12.0 for Windows (SPSS, 2003).

3. Results and discussion

3.1 Winter 2009-10

3.1.1 Meteorological pattern

The mean air temperatures was -5.2 °C with a minimum value of -14.3 °C registered on 19th of December 2009 (Fig. 3a). This season was characterized by one short mild period, from December 6th to 10th, when the air temperature reached positive values with a maximum of +3.9 °C. The mean daily air temperature became constantly positive after 20th of April 2010. Concerning precipitations, the automatic weather station recorded a cumulative precipitation equal to 330 mm of snow water equivalent (SWE). The maximum snow depth (135 cm) was reached on 2nd of April 2010.

The cumulative snowfall was lower than the 75 years historical data (488 mm of SWE) reported by Mercalli et al. (2003): in particular, the difference was remarkable especially during January, February and April.

3.1.2 Snow physical characteristics

In the *Larch plot*, the measured snow depth reached a maximum of 60 cm on January 13th.The snow density ranged between 184 kgm^{-3} (on January 13th) and 362 kgm^{-3} (on March 3rd). The first snow profile (December 9th) shown an isothermal snowpack with a basal layer characterized by slush crystals (MFsl). From the middle of December to the middle of February the thermal gradient increased and determined the formation of faceted crystals (MCso) and depth hoar (DHcp). In March the snowpack was again mostly at isothermal conditions with a predominance of melt-freeze crusts (MFcr).

The maximum snow depth measured in the *Spruce plot* (66 cm) was reached on February 2nd.The snow density ranged between 163 kgm^{-3} (on December 22nd) and 296 kgm^{-3} (on March 3rd). From the middle of December till the middle of February the thermal gradient increased and determined the formation of faceted crystals (MCso) and depth hoar (DHcp). In March the snowpack reached isothermal conditions with a predominance of cluster rounded crystals (MFcl).

3.1.3 Temperature and moisture at the snow/soil interface

In the *Larch plot*, the temperature at the snow/soil interface T_i (Fig. 3b) was positive until December 10th, except on November 29th, when a first freezing event occurred (daily average T_i = -1.3 °C). Later T_i remained below 0 °C from the middle of December until the end of March. A sharp increase of T_i (which reached 0 °C) was observed on December 26th, January 1st, February 19th, March 3rd and March 18th. The moisture at the snow/soil interface M_i (Fig. 3c) was correlated with the soil ($r = +0.498$; $p < 0.01$) and air temperatures ($r = +0.418$; $p < 0.01$). The maximum values were recorded several times during this winter season and in particular on December 8th (21%), with a wetting rate of 2%/day for 11 days, on December 25th (20%), with a wetting rate of 15% in one day and on February 26th (22%) with a wetting rate of 5%/day for 2 days. The period between the beginning of January and the middle of February was characterized by a constant value of M_i close to 10%.

In the *Spruce plot* the temperature at the snow/soil interface T_i (Fig. 3b) was positive until November 29th (T_i = -0.8 °C). Later T_i remained constantly below 0 °C from the middle of December until the end of March. The moisture at the snow/soil interface M_i (Fig. 3c) showed remarkable oscillations until the beginning of January, with 3 maximum values recorded on November 16th (14%), with a wetting rate equal to 2.5%/day for 4 days, on December 11th (15%), with a wetting rate of 1%/day for 14 days and on December 25th (13%), with a wetting rate of

274 6.5%/day for 2 days. Later, M_i remained constant (around 5%) until March 19th. From March 19th to
275 24th a remarkable increase was observed (+3.2%/day), reaching a moisture value of 21.3% on
276 March 24th. M_i was correlated with T_i ($r = +0.641$; $p < 0.01$) and air temperature ($r = +0.631$, $p <$
277 0.01).

278 3.1.4 Snow gliding

279 While not any snow gliding event was observed in the *Spruce plot*, in the *Larch* one, only a single
280 event of snow gliding occurred (Fig. 3d) between December 1st and 14th after the first seasonal
281 snowfall of 30 cm. In this period, M_i rose by 20% and the dominant grain type in the basal layer
282 observed on December 9th was slush (MFsl), indicating a consistent presence of liquid water. The
283 cumulative movement of the glide shoes was equal to 19 mm, with an average daily snow gliding
284 rate of 1.9 mm/day for 10 days and a maximum daily snow gliding rate of 3.9 mm/day. The
285 volumetric moisture at the snow/soil interface increased with a wetting rate +3.8%/day for 5 days.
286 From the middle of December until the end of the monitoring period, no snow gliding was
287 observed, although a significant increase of snow/soil interface temperature and moisture was
288 recorded at the end of March (wetting rate of +1.5 % day for 12 days).
289

290 3.1.5 Snow forces

291 In the *Larch plot*, the snow forces on stems with different diameters, calculated by Equation 3, as
292 in Margreth et al. (2007), ranged from 3 to 290 N (Fig. 4a). Two maximum values were calculated:
293 the first at the middle of January (H_S = 60 cm and ρ snow = 184 kgm^{-3}) and the second at the
294 beginning of March (H_S = 47 cm and ρ snow = 362 kgm^{-3}).
295 We also calculated the snow forces as in Mc Clung and Larsen (1989), in correspondence of the
296 single snow gliding episodes (beginning of December), when a movement of 3.9 mmday^{-1} was

297 registered by the snow shoes. The necessary input values for the snow depth and density were taken
298 from the snow pit dug on 9th of December: H_S = 25 cm and ρ snow= 250 kgm^{-3}. The resulting
299 forces ranged from 11 to 284 N on the different stem diameters (Tab. 2).
300
301 In the *Spruce plot* the snow forces on stems with different diameters, calculated by Equation 3, as
302 in Margreth et al. (2007), ranged from 2 to 361 N (Fig. 4b). A maximum was observed at the
303 middle of February, when H_S was equal to 66 cm and ρ snow 231 kgm^{-3}.
304 During winter 2009-2010, it was not possible to calculate the snow forces as in Mc Clung and
305 Larsen (1989), as no snow gliding event occurred under Spruce.
306
307 3.2 Winter 2010-11
308 3.2.1 Meteorological pattern
309 In winter 2010-11 the mean air temperatures was -3.0 °C with a minimum value of -14.3 °C
310 recorded on 18th of December (Fig. 3). Winter 2010-11 was characterized by frequent and longer
311 mild periods than winter 2009-2010. The mean daily air temperature became constantly positive
312 from 22nd March. Concerning precipitations, the automatic weather station recorded a cumulative
313 precipitation equal to 298 mm of snow water equivalent (SWE). The maximum snow depth (156
314 cm) was reached on 17th March 2011.
315 The cumulative snowfalls was lower than the 75 years historical data (488 mm of SWE) reported by
316 Mercalli et al. (2003): in particular, the difference was remarkable especially during January,
317 February and April.

318 3.2.2 Snow physical characteristics

319 In the *Larch plot*, a maximum snow depth equal to 28 cm was observed on December 2nd . The
320 snow density ranged between 146 kgm^{-3} (on December 2nd) and 340 kgm^{-3} (January 18th). The first

snow profile shown a kinetic methamorphism with the presence of faceted crystals (FCso), which we found also on January 18th. Moreover the dominant grain type in the basal layer was rounded polycrystals (MFpc) suggesting a previous presence of liquid water. On March 23rd a prevalence of cluster rounded crystals (MFcl) was observed.

In the *Spruce plot*, the maximum snow depth was observed in the last snow profile (28 cm) on March 23rd. The snow density ranged between 230 kgm^{-3} (on December 2nd) and 320 kgm^{-3} (January 18th). The first snow profile revealed the beginning of kinetic metamorphism, with faceted crystals (FCso) as prevalent crystals; moreover a thin ice layer (IFil) was observed at the bottom of the snowpack. On March 23rd a prevalence of rounded crystals (RGlr) was observed.

3.2.3 Temperature and moisture at the snow/soil interface

The temperature sensors in the *Larch plot* were repeatedly damaged by rodents, therefore the measurements were interrupted. The recorded T_i values ranged only from November to December and from the end of January until the middle of February (Fig. 3b).

The moisture at the snow/soil interface M_i (Fig. 3c) was characterized by 4 sharp increases: the first (34%) occurred from November 14th to 16th (wetting rate: +12%/day); the second (34%), occurred from December 5th to 9th (wetting rate: +9%/day); the third (37%) occurred from January 13th to 16th (wetting rate: +5%/day); the fourth (32%), occurred from March 13th to 20th (wetting rate: +4%/day). On the contrary, M_i strongly decreased (-25%) from November 21th until December 4th, with a drying rate equal to -1.8%/day. M_i was positively correlated with the air temperature ($r = +0.256$; $p < 0.01$).

In the *Spruce plot* the temperature at the snow/soil interface T_i (Fig. 3b) was constantly negative from November 24th until March 3rd, except three periods when it reached 0 °C (December 8th, January 14th to 18th and February 6th to 11th). Two minimum values were reached, on December 18th

(-4.6 °C) and January 21th (-4 °C). When the snow/soil interface temperature increased, also the moisture M_i did (r = +0.650 p<0.01), and the maximum values, 42%, 49% and 33%, were reached on November 16th, January 15th and February 9th , respectively (Fig. 3c). Instead, the minimum water content measured in the Spruce plot (0%) was reached at the beginning of December when the snow/soil interface was frozen.

3.2.4 Snow gliding

In the *Larch plot*, several snow gliding events were measured with a cumulative movement of 77 mm (Fig. 3d).

The first snow gliding event was recorded after the first snowfall (25 cm) at the end of November. From November 13th to November 23rd a cumulative movement of 43 mm was recorded. In this period, *Ti* was positive (daily average T_i = 1.4 °C) and a remarkable snow/soil moisture increase (+ 7.4%/day for 3 days) occurred. The highest snow gliding rate (1.4 mm/day) was measured on November 17th. In the snow profile dug closer in time to this snow gliding event (December 2nd) the dominant grain type in the basal layer was rounded polycrystals (MFpc), indicating that melt-freeze metamorphism occurred, with the presence of some liquid water.

Until the middle of January, the snow gliding rates decreased, with a cumulative value equal to 5.8 mm. From January 19th till April 4th other snow gliding events were observed (for a cumulative movement of 29 mm): the highest daily movement was recorded on January 20th (0.4 mm/day) and on March 3rd (0.1 mm/day), after a significant increase of M_i (respectively +2.4/day for 7 days and +8.7 in one day). Especially on January 18th an increase in snow moisture across the snow pack was observed: the basal layer contained a significant amount of liquid water. No snow gliding was observed from February 6th until 16th because the study plot became snow free.

In the *Spruce plot*, only a single snow gliding event was observed, after the first snowfall, with a cumulative displacement of 16 mm, from the 13th to the 25th November. In the snow profile dug closer in time to this snow gliding event (December 2nd) a thin ice layer (IFil) was observed at the bottom of snowpack indicating a previous presence of some liquid water at the snow/soil interface. The highest snow gliding rate (0.4 mm/day), was measured on November 19th, after a significant increase of the volumetric moisture (+4.75/day for 3 days). From the end of November until the end of the monitoring period, no snow gliding was observed, despite several increments at the snow/soil interface moisture were recorded.

3.2.5 Snow forces

In the *Larch plot*, the snow forces on stems with different diameters calculated by Equation 3 (as in Margreth et al., 2007) ranged from 0.5 to 29 N (Fig. 5a). The snow forces decreased from the beginning of December (H_S = 28 cm; ρ snow= 146 kgm^{-3}) to the beginning of January (H_S = 10 cm; ρ snow = 340 kgm^{-3}) and then remained almost constant until the end of the season. Also according to Mc Clung and Larsen (1989), the snow forces decreased across the season since the maximum snow gliding rate, 1.4 mmday^{-1}, was observed on November 17th and the minimum one, 0.1 mmday^{-1}, was measured on March 03rd. The resulting forces ranged from 2 to 184 N (Tab.2).

In the *Spruce plot*, the snow forces on stems with different diameters calculated by Equation 3 (as in Margreth et al., 2007) ranged from 0.6 to 21 N (Fig. 5b). The snow forces were almost constant until the beginning of January (H_S = 11 cm; ρ snow = 320 kgm^{-3}) and then started to increase until the end of March (H_S = 28 cm; ρ snow 260 kgm^{-3}). We also calculated the snow forces as in Mc Clung and Larsen (1989), in correspondence of the single snow gliding episode (second half of November), when a movement of 0.4 mm was registered by the snow shoes. The necessary input values for the snow depth and density were taken from the snow pit dug on December 2nd: H_S = 20

392 cm and ρ snow= 232 kgm^{-3}. The resulting forces ranged from 3 to 66 N on the different stem
393 diameters (Tab. 2).
394
395 3.3 Comparison between Larch and Spruce plots
396 3.3.1 Snow physical characteristics
397 From our results, it seems that the tree species affect only some physical characteristics of the
398 snowpack. In fact, the crystal type and dimension were similar both under Larch and Spruce stands.
399 Instead, the snow depth evolution had a different pattern within the two sites: in full winter,
400 snowfalls generated a deeper snowpack in the Larch plot, because of the reduction of snow
401 interception due to the absence of leaves in the winter period; on the contrary, in spring, the shadow
402 effect due to the evergreen cover maintained a deeper snowpack and increased the snow duration
403 under the Spruce plot. The same effect of crown interception was found by Gubler and Rychetnik
404 (1991) and Motta (1995).
405 A higher average snow density was observed under Spruce, especially after snowfalls with mild air
406 temperature, maybe due to the liquid water input from the melted snow intercepted by the tree
407 crowns. The snow density under Larch gradually increased and exceeded the values recorded under
408 Spruce, when the direct solar radiation during spring time became relevant.

409 3.3.2 Temperature and moisture at the snow/soil interface
410 The mean snow/soil interface temperature was higher within the Larch than within the Spruce plots,
411 especially during fall and spring. An explanation could be that the greater snow accumulation under
412 Larch during early winter, when the soil was unfrozen, could have reduced the soil cooling rate,
413 while the higher snow depth in the Spruce plot in late winter and spring could have determined a
414 delay in the soil warming. Several authors (e.g. Brooks and Williams 1999; Freppaz et al. 2008)

found that approximately a snow depth equal to 30-40 cm accumulating early in the winter season prevents soil from freezing.

Concerning the moisture at the snow/soil interface, we registered larger fluctuations in the Larch than in the Spruce plot. The reason might be that a lower crown cover permitted the irradiation to reach the snowpack surface. This energy input increased the snow water content at the surface, which, due to a thin snowpack, was able to percolated until the ground. On the contrary, in the Spruce plot, the larger crown cover made the influence of the irradiation negligible.

3.3.3 Snow gliding

In both years the total snow gliding was higher under Larch than under Spruce. This fact was probably due to a lower snowpack basal friction under Larch than under Spruce, caused by great fluctuations of moisture at the snow/soil interface. The cumulative snow gliding did not exceed 100 mm, as found also by Höller (2001) for a dense forest. This result confirmed that snow gliding is generally low when the canopy density is relatively high.

3.3.4 Snow forces

Generally, lower forces were calculated below Spruce than below Larch, due to the larger snow accumulation recorded in the latter site. We did not find any damages to young trees in both plots.

4 General discussion

From our results, the snow/soil interface moisture significantly influenced the snow gliding processes. In particular the water content at the snow/soil interface was related to the snow/soil interface temperature; moreover, it resulted strongly positively correlated with air temperature. It seemed that the velocity of the wetting front in the snowpack was strongly influenced by air temperature and snow depth, with a contrasting effect: higher air temperature and lower snow depth

let the wetting front to move faster within the snowpack. Jones et al. (2001) also suggested that peak discharges from a snowpack with flow instabilities could be much higher and faster if the pack was homogeneous. In fact, we found that during early winter, when the snow cover was thin and homogeneous (mainly characterized by fresh snow) the volumetric moisture at the bottom increased in less than 24 hours under both plots after the increase of air temperature. Instead, during full winter, when the snowpack was thicker, after an increase of air temperature, the snow/soil interface moisture increased due to the wetting front from the surface (which reached the bottom of the snow cover within a maximum of 4 days) but also due to the increase of the snow/soil interface temperature (which reached 0 °C).

The volumetric moisture increase of a relatively dry snow/soil interface (10-20%), seemed to be the most important factors influencing the snow gliding rates: in particular snow gliding was observed with wetting rates higher than 1.2%/day. The increase of volumetric moisture at the snow/soil interface might reduce the snowpack basal friction as suggested by several authors (In der Gand 1966; Clarke and Mc Clung 1999; Höller 2001; Margreth et al. 2007). The snow gliding events were mostly recorded, under both plots, during early winter and after the first snowfalls, when the soil was unfrozen, as observed also in long term studies, though done in open field (In der Gand and Zupancic 1966; Hoeller 2001). The first snow at ground melted on mild soil (T_i > 0.5 °C), thus determining an increase of moisture at the snow/soil interface, where the dominant crystal type was slush. During winter 2010-11, snow gliding events were observed also during spring time. These phenomena were related to a sudden sharp air temperature increase, which consequently increased the snowpack moisture, followed by a strong air temperature decrease, as observed by McClung (1999). We could hypothize that the snowpack became stiff and glided, as a block, on the liquid water film previously formed at the soil surface.

The calculated snow forces were lower than the values reported in other studies in the Alps (Höller et al. 2009). The differences could be attributed to the lower coefficients we used, because our study

site was located under a mature forest stand, while the study site considered for example by Höller et al. (2009) was characterized by young trees. Moreover, our study site was characterized by lower slope angle and lower snow density and thickness than the site studied by Höller et al. (2009).

With our data, the application of the method by Margreth et al. (2007), originally elaborated for the dimensioning of the cableway masts, gave lower values than the method by Mc Clung and Larsen (1989), and the differences between the two methods became more significant with larger stem diameters. This difference suggests to directly measure the snow forces by using load cells on the tree trunks, in order to validate the results obtainable with the two different methods.

The fact that we did not survey any damages to young trees, such as seasonal uproots and branch breakages, is in agreements with the low snow forces obtained with the two different methods. Our calculated snow forces were lower than the value of 950 N, found by Höller (2009), through pulling test, as the minimum force necessary to cause uprooting of young coniferous trees (*Larix decidua, Picea abies e Pinus cembra*), with stem diameters ranging from 2.5 to 5 cm.

However, the snow characteristics (e.g. density) and meteorological conditions (e.g. sharp increase of air temperature) recorded during the two winters considered in this study, caused significant snow gliding events, mainly during early winter, which contributed to determine not transcurable snow forces on trees, though not producing damages.

Since the Climate change is expected to determine milder winter and more unstable snow cover in temperate mountain regions (Cooley 1990; IPCC 2007), it is possible to speculate a change also in the snow gliding processes. In particular, these areas could face a decline in snow cover (late snowpack accumulation and advance of snowmelt timing), an increase of snow density and more frequent episodes of rain on snow (Leung et al. 2004; Ye et al. 2008; Casson et al. 2010). Hence, the basal friction of the snowpack could be reduced by the liquid water on the basal portion of the snowpack and consequently amplify the rate of snow gliding. This fact might generate in future higher pressure on stems diminishing trees stability and therefore the forest protective function.

5 Conclusion

In this work we evaluated the snowpack physical characteristics, we measured the properties at the snow/soil interface, the snow gliding and we calculated the snow forces on trees of different species and diameters. In particular we observed that:

a) The snowpack physical evolution (e.g. snow density, snow depth) during the whole winter season was influenced by the tree species, due to the different crown interception of snowfall, and the different degree of exposure of the snowpack to the incoming solar radiation;

b) The wetting rate at the snow/soil interface, related with the air temperature, seemed to be the most important factor influencing the snow gliding rates. The snow gliding rates seemed to be higher in early winter, when the first snowfall covers an unfrozen soil. In this period, snow gliding was observed after the wetting of a relatively dry snow/soil interface (moisture 10-20%) when the increase of moisture exceeded +1.2%/day and the interface temperature was >0.5°C;

c) The highest snow gliding was measured under the Larch stand;

d) The calculated snow forces were very low under both forest stands, if compared to other studies, mainly because the snow depth and the snow density were scanty during the study period;

e) According to the Climate change scenarios, it was possible to hypothesize an increase of the snow gliding rates due to a higher moisture at the snow/soil interface.

Acknowledgements

This study was possible thanks to the Project “Forêts de protection: techniques de gestion et innovation dans les Alpes occidentals” within the Operational Program ALCOTRA Italy-France 2009-2012)”.

Many thanks to Franca De Ferrari, Jean–Claude Haudemand, Antoine Brulport, Franco Viglietti and Gianluca Filippa for the important contribution in field activities and data elaboration.

References

Bader, H., R. Haefeli, E. Bucher, I. Neher, O. Eckel and Chr. Thams. 1939. Der Schnee und seine Metamorphose (Snow and its Metamorphism). Beitrage zur Geologie der Schweiz, Geotechnische Serie, Hydrologie, Lieferung 3, Bern [English Translation by Snow, Ice Permafrost Research Establishment, Corps of Engineers, U.S. Army. Translation 14, January 1954], 313 pp.

Brooks, P.D., Williams, M.W. 1999. Snowpack controls on nitrogen cycling and export in seasonally snow-covered catchments. *Hydrol. Process.* **13**:2177–2190.

Casson, N.J., Eimers, M.C., Buttle, J.M. 2010. The contribution of rain-on-snow events to nitrate export in the forested landscape of south-central Ontario, Canada. *Hydrol. Process.* **24**:1985-93.

Clarke, J., Mc Clung, D. 1999. Full depth avalanche occurrences caused by snow gliding, Coquihalla, British Columbia, *Canada. J. Glaciol.* **45**(150):539-546.

Cooley, K.R. 1990. Effects of CO2-induced climate changes on snowpack and streamflow. *Hydrol. Sci. J.* **35** :511-522.

Freppaz, M., Marchelli, M., Celi, L., Zanini, E. 2008. Snow removal and its influence on temperature and N dynamics in alpine soils (Vallée d'Aoste - NW Italy). *J. Plant Nutr. Soil Sci.* **171**:1-9.

555 Fierz, C., Armstrong, R.L., Durand, Y., Etchevers, P., Greene, E., McClung, D.M., Nishimura, K.,
556 Satyawali, P.K., Sokratov, S.A. 2009. *The International Classification for Seasonal Snow on the*
557 *Ground*. IHP-VII Technical Documents in Hydrology N°83, IACS Contribution N°1, UNESCO-
558 IHP, Paris.
559
560 Gubler, H., Rychetnik, J. 1991. Effect of forests near the timberline on avalanche formation. Snow
561 Hydrology and Forest in High Alpine Areas (Proceeding of Vienna Symposium, August 1991).
562 IAHS Publ.205, 1991.
563
564 Höller, P., Fromm, R., Leitinger, G. 2009. Snow Forces on Forest Plants Due To Creep And Glide.
565 *For. Ecol. Manag.* **257**:546-552.
566
567 Höller, P. 2001. Snow gliding and avalanches in a south-facing larch stand. *Intern. Ass. Hydrol. Sci.*
568 *Publ.* **270**:355–358.
569
570 In der Gand, H., Zupancic, M. 1966. Snowgliding and avalanches. Scientific Aspects of Snow and
571 Ice Avalanches (Proceeding Davos Symposium, April 1965), 230-242 . IAHS n.69.
572
573 In der Gand, H. 1954. Beitrag zum Problem des Gleitens der Schneedecke auf dem Untergrund.
574 Winterbericht Eidg. Inst. f. Schnee-und Lawinenforschung **17**:103–117.
575
576 In der Gand, H. 1978. Verteilung und Struktur der Schneedecke unter Waldbaumen und im
577 Hochwald. International Seminar on Mountain Forests and Avalanches. IUFRO Working Party on
578 Snow and Avalanches. Davos: Swiss Federal Institute for Snow and Avalanche Research, 98–119.
579

IPCC Intergovernmental Panel on Climate Change (IPCC) 2007. Climate Change 2007: The Physical Science Basis: Working Group 1 Contribution to the Fourth Assessment Report of the IPCC, edited by S. Solomon, D. Qin, and M. Manning, Cambridge Univ. Press, New York.

Jones, H.G., Pomerow, J.W., Walker, D.A., Hoham, R.W. 2001. *Snow Ecology: an interdisciplinary examination of snow covered ecosystems.* Cambridge University Press, pp. 102-104.

Jones, A. 2004. Review of glide processes and glide avalanche release. *Avalanche News* **69**: 53–60.

Lackinger, B. 1987. Stability and fracture of the snow pack for glide avalanches. *Intern. Ass. Hydrol. Sci. Publ.* **162**:229–240.

Leitinger, G., Höller, P., Tasser, E., Walde, J., Tappeiner, U. 2008. Development and validation of a spatial snow-glide model. *Ecol. mod.* **211**:363–374.

Leung, L., Qian, Y., Bian, X., Washington, W., Han, J., Roads, J. 2004. Mid-century ensemble regional climate change scenarios for the western United States RID A-5056-2010. *Clim. Ch.* **62**: 75-113.

Margreth, S. 2007a. Defense structures in avalanche starting zones. *Technical guideline as an aid to enforcement.* Environment in Practice no. 0704. Federal Office for the Environment, Bern; WSL Swiss Federal Institute for Snow and Avalanche Research SLF, Davos, 134 pp.

Margreth, S. 2007b. Snow pressure on cableway masts: analysis of damages and design approach. *Cold Reg. Sci. Technol.* **47**,4–15.

McClung, D.M. and G.K.C. Clarke. 1987. The effects of free water on snow gliding. *J. Geoph. Res.* **92**(7): 6301-6309.

McClung, D., Larsen, J.O. 1989. Snow creep pressure: effect of structure boundary conditions and snowpack properties compared with field data. *Cold Reg. Sci. Technol.* **17**:33-47.

Mercalli, L., Catberro, D., Montuschi, S., Castellano, C., Ratti, M., Di Napoli, G., Mortara, G., Guindani, N. 2003. Atlante Climatico della Valle D'Aosta (Climate Atlas for the Aosta Valley Region) (Eds. Società Meteorologica Subalpina) 405 pp.

Motta, R. 1995. I lariceti delle Alpi occidentali: un problema ecologico selvicolturale. SILVAE pedemontis **1**:7–16.

Newesely, C,. Spadinger, P., Cernusca, A., Tasser, E. 2000. Effects of land-use changes on snow gliding processes in alpine ecosystems. *Bas. Appl. Ecol.* **1**: 61–67.

Salm, B. 1977. Snow forces. *J. Glaciol*. **19**(81):67–100.

SPSS 2003. SPSS for Windows. SPSS Inc., Chicago.

Tasser, E., Newesely, C., Höller, P., Cernusca, A., Tappeiner, U. 1999. Potential risks through land-use changes. ECOMONT. Ecological effects of land-use changes on European Terrestrial Mountain Ecosystems – Concepts and Results. Blackwell Wiss.-Ver., Berlin, Wien. P 218–224.

630 Tasser, E., Tappeiner, U., Cernusca, A. 2001. Südtirols Almen im Wandel. Ökologische Folgen von
631 Landnutzungsänderungen. European Academy of Bozen/Bolzano 28, Bozen, p 276.
632
633 Tasser, E., Walde, J., Tappeiner, U., Teutsch, A., Noggler, W. 2007. Land-use changes and natural
634 reforestation in the Eastern Central Alps. *Agr. Ecosyst. and Envir.* **118**:115–129.
635
636 Valinger, E., Lundqvist, L. 1994. Reducing wind and snow induced damage in forestry. Swedish
637 University of Agricultural Sciences. Department of Silviculture. Reports 37.
638
639 Viglietti, D., Letey, S., Motta, R., Maggioni, M., Freppaz, M. 2010. Snow avalanche release in
640 forest ecosystems: A case study in the Aosta Valley Region. *Cold Reg. Sci. Technol.* **64**(2):167-173.
641
642 Ye, H., Yang, D., Robinson, D. 2008. Winter rain on snow and its association with air temperature
643 in northern Eurasia. *Hydrol. Process.* **22**:2728-36.
644
645
646
647
648
649
650 **Figure captions**
651
652 **Fig. 1** Localization of the study site and of the two selected plots
653

654 **Fig. 2** Moisture (a) and temperature (b) sensors, and a glide shoe (c), connected to the
655 potentiometer, used in the study site
656
657 **Fig. 3** Snow depth and air temperature measured by the automatic snow and weather station (a); *Ti*
658 (b) *Mi* (c) and snow gliding (d) in each plot recorded in both the seasons (2009-10 and 2010-11)
659 when the study site was covered by snow
660
661 **Fig. 4** Snow forces calculated according to Margreth et al. (2007) at different stem diameters during
662 winter 2009-10 in the Larch (a) and Spruce plots (b)
663
664 **Fig. 5** Snow forces calculated according to Margreth et al. (2007) at different stem diameters during
665 winter 2010-11 Larch (a) and Spruce (b) plots
666
667
668
669
670
671
672
673

m. Figures captions

Fig. 1: Localization of the study site and of the two selected plots.

Fig. 2: Moisture (a) and temperature (b) sensors, and a glide shoe (c), connected to the potentiometer, used in the study site.

Fig. 3: Snow gliding and snow/soil interface volumetric moisture (M_i) recorded under Larch during winter 2009-10.

Fig. 4: Snow gliding and snow/soil interface volumetric moisture (M_i) recorded in all plots in winter 2010-11.

Fig.5: Snow forces calculated according to Margreth et al. (2007) at different stem diameters during winter 2009-10 in the Larch (a) and Spruce plots (b).

Fig.6: Snow forces calculated according to Margreth et al. (2007) at different stem diameters during winter 2010-11 Larch (a) and Spruce (b) plots.

Fig.7: Snow forces under the Larch plot on December 4th, 2009, calculated with the two different methods (Margreth et al., 2007 and Mc Clung and Larsen, 1989).

702

703

704

705

706

707

n. Figures

Fig.1

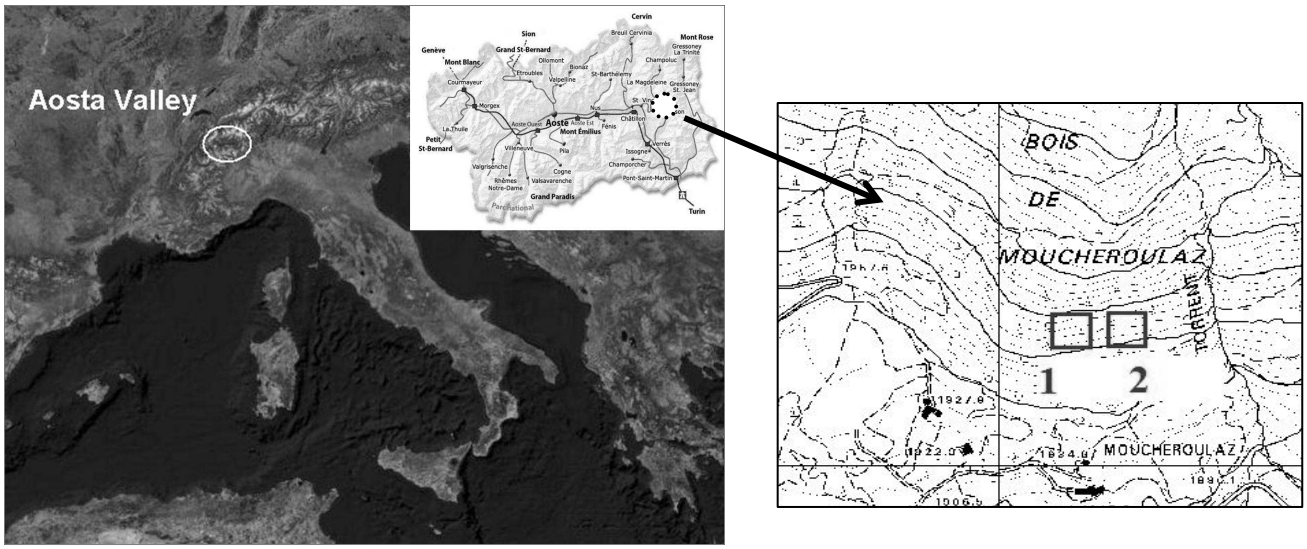

Fig. 2

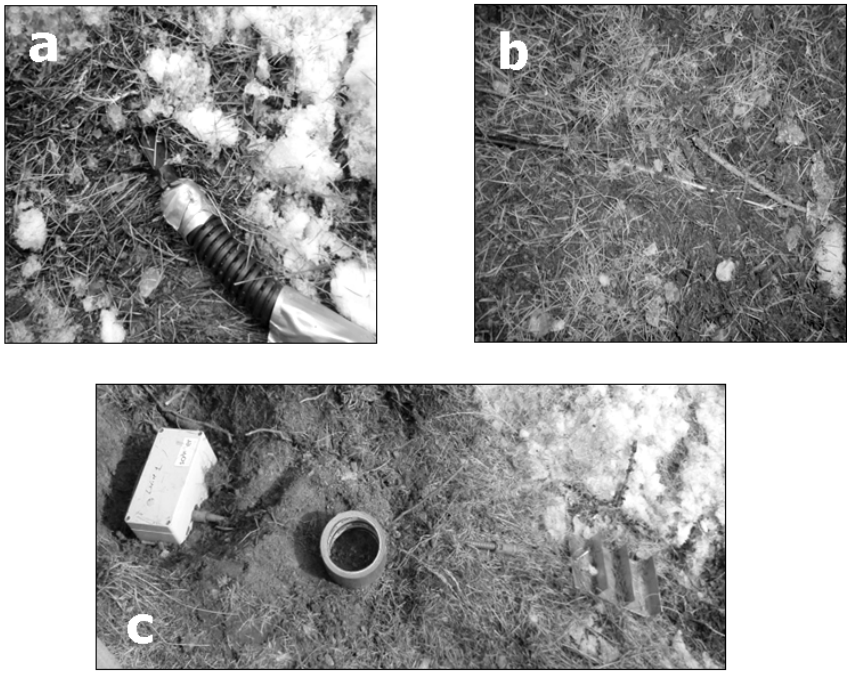

752

753

754

755

756

757

758

759

760

761

762

763

764

765

766

767

768

769

770

771

772 Fig. 3

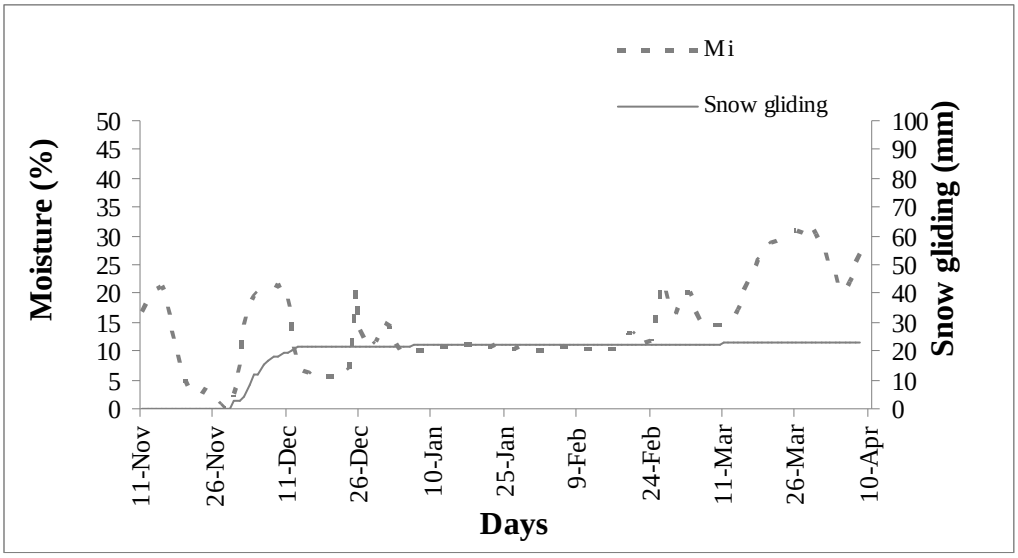

773

774

775

776

777

778

779

780

781

782

783

784

785

786

787

788

789

790

Fig. 4

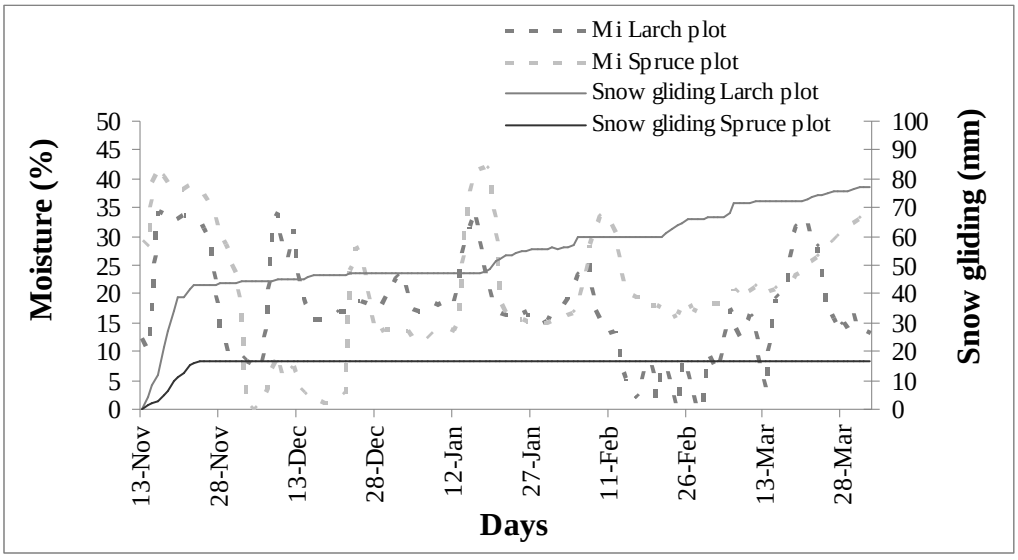
Mi Larch plot
Mi Spruce plot
Snow gliding Larch plot
Snow gliding Spruce plot
Moisture (%)
Snow gliding (mm)
Days
13-Nov
28-Nov
13-Dec
28-Dec
12-Jan
27-Jan
11-Feb
26-Feb
13-Mar
28-Mar

807

808

Fig. 5

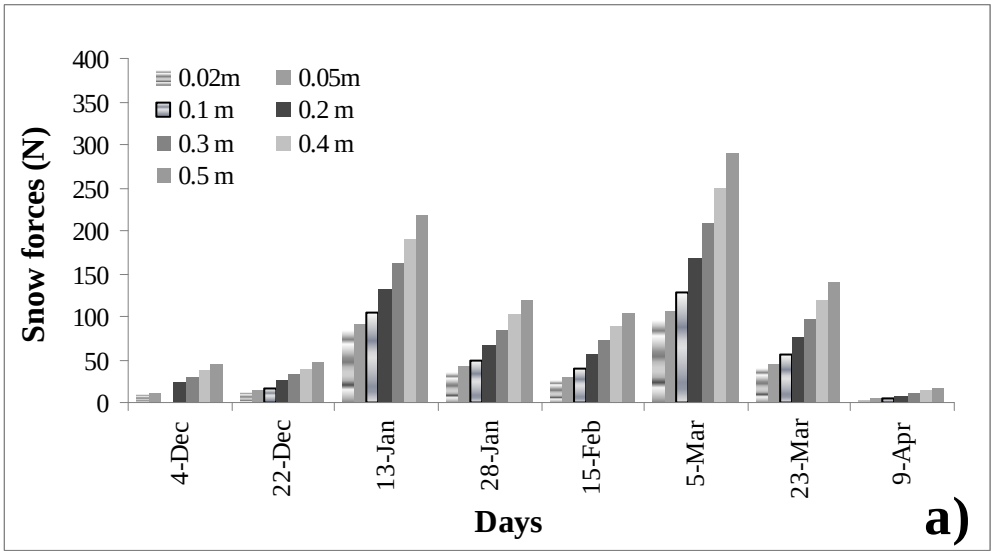
Snow forces (N)
400
350
300
250
200
150
100
50
0
0.02m
0.05m
0.1 m
0.2 m
0.3 m
0.4 m
0.5 m
4-Dec
22-Dec
13-Jan
28-Jan
15-Feb
5-Mar
23-Mar
9-Apr
Days
a)

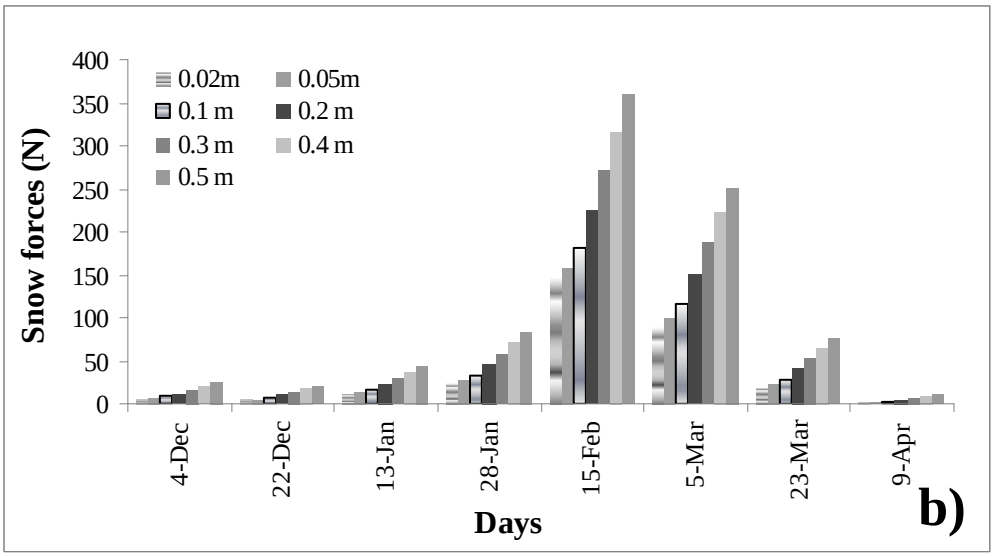
Snow forces (N)
400
350
300
250
200
150
100
50
0
0.02m
0.05m
0.1 m
0.2 m
0.3 m
0.4 m
0.5 m
4-Dec
22-Dec
13-Jan
28-Jan
15-Feb
5-Mar
23-Mar
9-Apr
Days
b)

828 Fig. 6

829

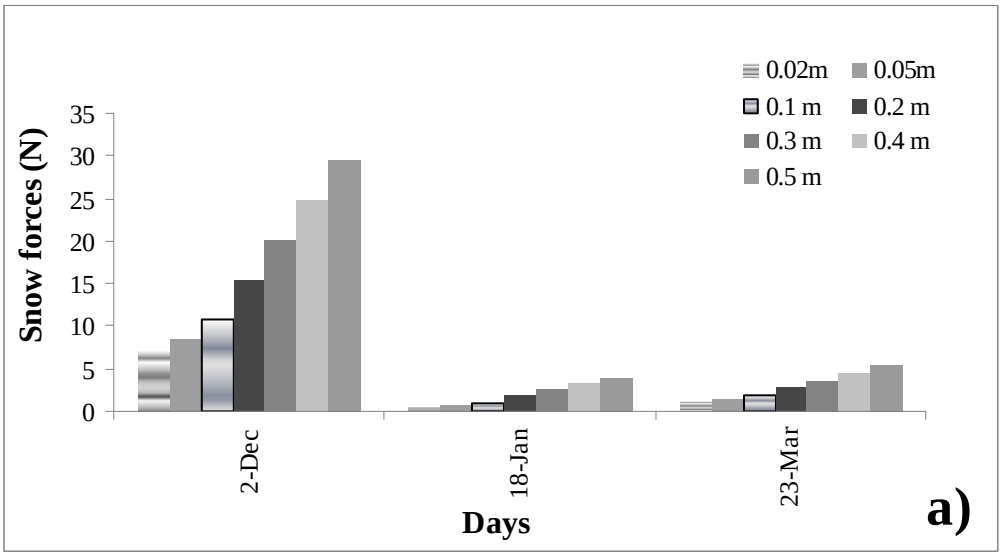

830

831

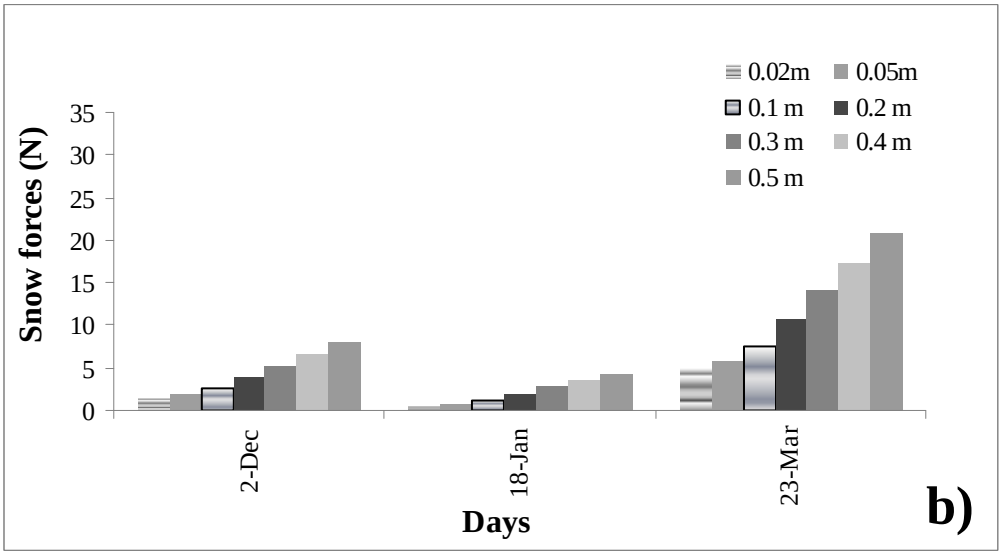

832

833

834

835

836

837

838

839

840

841

842

843

844

845

846

847

848

849 Fig. 7

850

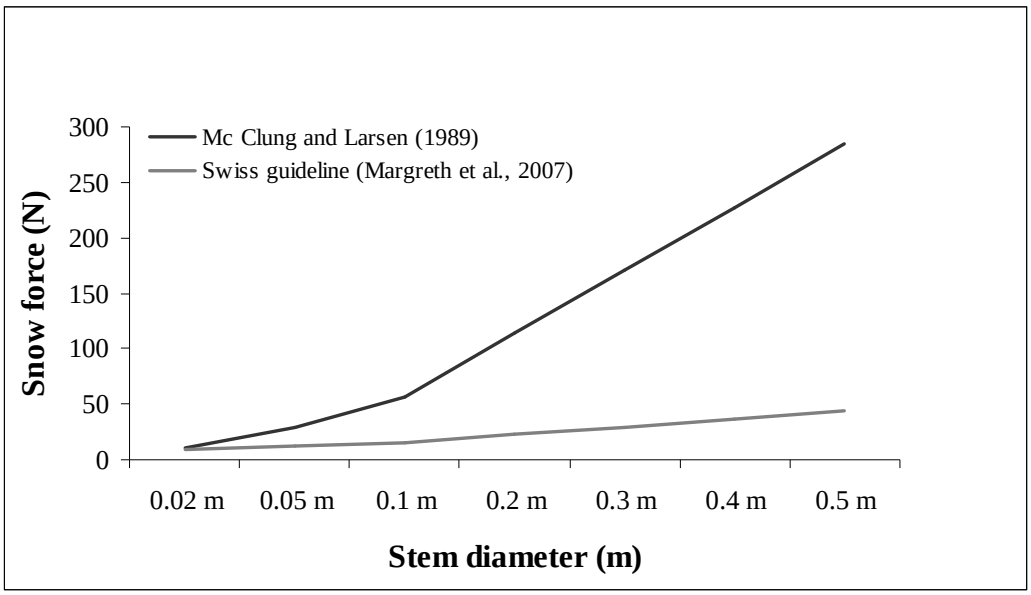

851

852

853

854

855

856

857

858

859

860

861

862

863

864

865

866 l. Tables

867 Tab.1: Mean values of the physical snow properties (according to Fierz et al., 2009) measured in the
868 field during winter 2009-10 (8 snow profiles) and 2010-11 (3 snow profiles), under Larch (L) and
869 Spruce (S) plots. Modal values are shown for categorical variables marked with an asterisk (*).

870

	2009-10		**2010-11**	
Parameter	**L**	**S**	**L**	**S**
Maximum value of snow depth (cm)	60	66	28	22
*Grain type in basal layer	FC_{so}, DH_{cp}	DH_{cp}	FC_{so}	FC_{so}
*Dominant grain	FC_{so}, MF_{pc}	FC_{so}, DH_{cp}	RG_{sr}	RG_{sr}
Maximum grain size (mm)	2.5	4	1.5	1.5
Hand hardness Index	3	4	3	2
Snow/soil interface temperature (°C)	-3.8	-2.1	-1.1	-1.8
Date of isothermal condition	March 11rd	March 19rd	March 14rd	March 20rd
Snow density (kg/m^3)	277	229	220	270

871

872

873 Tab.2: Values of T_i and M_i (standard deviations) averaged over the respective meteorological
874 seasons in 2009-10 and 2010-11. Also the mean air temperature is shown.

875

876

877

	2009-10					
	Fall		**Winter**		**Spring**	
	T_i (°C)	**M_i (%)**	**T_i (°C)**	**M_i (%)**	**T_i (°C)**	**M_i (%)**
L	2.1 (2.4)	8.5 (8.6)	-2.2(1.8)	11.8 (4.1)	-0.4 (1.2)	23.0 (6,0)
S	1.4 (1.7)	6.8 (4.5)	-2.7 (1.8)	4.7 (2.9)	-1.3 (1.4)	13.1 (8,2)
Air	2.0 (3.1)		-5.1 (3.6)		-1.9 (4.2)	
	2010-11					
	Fall		**Winter**		**Spring**	
	T_i (°C)	**M_i (%)**	**T_i (°C)**	**M_i (%)**	**T_i (°C)**	**M_i (%)**
L	0.5 (1.7)	25.5 (9.9)	--	16.4 (6.8)	--	16.7 (8.2)
S	0.3 (1.8)	34.8 (5.0)	-1.5 (1.3)	16.5 (10.7)	-0.4 (0,3)	24.1 (5.2)
Air	-3.9 (5.0)		-3.1 (4.2)		0.3 (4)	

878

879

880

881 Tab.3: Snow forces values calculated according to Mc Clung and Larsen (1989) for the winter
882 2009-10 for the different stem diameter classes under Larch.

883

884

885

886

Date and snowgliding rates	Forces at different diameter classes (N)						
	0.02 m	0.05 m	0.1 m	0.2 m	0.3 m	0.4 m	0.5 m
887 December 4th, 3.9mm/day	11.37	28.43	56.86	113.72	170.58	227.47	284.30

Tab.4: Snow forces values calculated according to Mc Clung and Larsen (1989) for the winter 2009-10 for the different stem diameter classes under Larch (L) and Spruce (S).

	L						
Date and snowgliding rates	**Forces at different diameter classes (N)**						
	0.02 m	0.05 m	0.1 m	0.2 m	0.3 m	0.4 m	0.5 m
November 17th, 1.4 mm/day	7.38	18.46	36.92	73.83	110.75	147.66	184.54
January 20th, 0.4 mm/day	2.55	6.39	12.77	25.55	38.32	51.10	63.87
March 03rd, 0.1 mm/day	1.82	4.54	9.08	18.17	27.25	36.34	45.42
	S						
Date and snowgliding rates	**Forces at different diameter classes (N)**						
	0.02 m	0.05 m	0.1 m	0.2 m	0.3 m	0.4 m	0.5 m
November 19th, 0.4 mm/day	2.62	6.56	13.11	26.22	39.33	52.45	65.56